

TWENTYFIFTH EUROPEAN ROTORCRAFT FORUM

Paper G-20

**Development of a Piezoelectrically Actuated Leading-Edge Flap
for Dynamic Stall Delay**

BY

**T. Lorkowski, P. Jänker, F. Hermle S.Storm, M. Christmann, M. Wettemann
DaimlerChrysler AG
Research & Technology
P.O. Box 800 465
81663 Munich
Germany**

**SEPTEMBER 14-16, 1999
R O M E
I T A L Y**

**ASSOCIAZIONE INDUSTRIE PER L'AEROSPAZIO; I SISTEMI E LA DIFESA
ASSOCIAZIONE ITALIANA DI AERONAUTICA ED ASTRONAUTICA**

DEVELOPMENT OF A PIEZOELECTRICALLY ACTUATED LEADING-EDGE FLAP FOR DYNAMIC STALL DELAY

T. Lorkowski, P. Jänker, F. Hermlle, S. Storm, M. Christmann
DaimlerChrysler AG, Research and Technology
Research Section Structural Materials, P.O. Box 800 465, 81663 Munich, Germany

The design of a rotor blade requires a multitude of compromises due to the highly unsteady conditions during helicopter flight. Continuous adaptation to the constantly changing aerodynamic environment, e.g. by means of a variable airfoil geometry, should help to substantially improve the performance, safety and comfort of future helicopters and enhance their acceptability. One operational constraint is the phenomenon of dynamic stall on the retreating blade under certain flight conditions. In situ dynamic high-lift devices integrated in the blade to delay this undesirable phenomenon demand a compact and rapid-response drive mechanism. High-performance piezoceramic actuators developed by DaimlerChrysler provide a promising solution to this problem. Based on the analysis and benchmarking of various dynamic high-lift devices, an approach was derived that appears suitable for piezoelectric actuators: dynamic nose droop, whose aerodynamic benefit has already been demonstrated. A design proposal for the structural integration of a leading-edge flap is presented. Numerical two-dimensional simulation using a conventional rotor airfoil led to a trade-off between aerodynamic efficiency and mechanical performance. Implementation of the design gives special consideration to aerodynamic sealing and low-friction mounting without play at the actuator/flap coupling.

1. INTRODUCTION

With their ability to take off and land vertically, helicopters have become indispensable in many areas, rescue missions, off-shore supply, and surveillance being classical examples. Comparatively high operating costs and high noise and vibration levels have so far been tolerated for the most part. However, because of their predominantly low-altitude operations, helicopters with their specific characteristics are increasingly perceived as environmental disturbances. Noise and vibrations reduce in-flight comfort for pilot and passengers. Vibrations also cause premature fatigue to humans and material and lead to higher inspection and maintenance costs. Noise reduction, higher in-flight comfort and an expanded operational envelope with enhanced performance are therefore urgently needed in order to open up new potential applications for this attractive and unique aircraft and improve its acceptance.

To meet all these requirements, new, intelligent concepts must be devised, as conventional technologies are already approaching their limits. The partners within the Adaptive Rotor Systems project (AROSYS) — Eurocopter Deutschland (ECD), the German Aerospace Center (DLR), and the Research and Technology Department of DaimlerChrysler — are working intensively to impart competitive characteristics to future helicopter generations [1]. Measures such as an active strut or a trailing-edge flap (servoflap) for individual blade control are prime examples [2].

In contrast to a fixed-wing aircraft, where lift, thrust and control are provided by three separate systems, in a helicopter the main rotor essentially provides all these functions required for controlled flight. The design of a rotor therefore entails a number of trade-offs. Consequently, any rotor blade will exhibit aerodynamic deficits in certain areas. One problem is the possible occurrence of flow separation on the retreating blade of the rotor. Known as dynamic stall, this can cause strong

vibrations as well as limiting the performance of the helicopter. A remedy is promised by active adaptation of the blade characteristics by means of dynamic high-lift devices.

2. DYNAMIC STALL

As a helicopter travels forward, vectorial superimposition of the forward and rotational speeds (V_∞ , Ω) produces higher velocities of the oncoming flow for the rotor blade on the advancing side of the rotor than on the retreating side. To ensure symmetric lift distribution, the angle of attack of the blade is therefore varied cyclically. The faster the helicopter travels forward, the more the blade must be inclined on the retreating side. When a certain point is reached, this leads to flow separation called dynamic stall within a locally limited area (Fig. 1).

The phenomenon of dynamic stall has been extensively investigated both numerically and experimentally [3]-[6]. Most of the studies have been restricted to the two-dimensional case. This paper additionally deals with what is known as "deep dynamic stall" only. Deep dynamic stall is characterized by distinct hysteresis loops in the aerodynamic force and moment coefficients (Fig. 2, left). If the amplitude of the angle-of-attack oscillation is sufficiently large, the maximum angle of attack of the blade is well above the static stall angle and the Mach number is relatively low, the phenomenon is largely independent of other parameters such as the blade geometry, type of motion, and Reynold's number.

Fig. 2 also shows the processes that occur during dynamic stall over one cycle. Once the static limits are exceeded during the oscillation, a reversed-flow area forms in the boundary layer starting at the trailing edge of the airfoil. The aerodynamic phenomenon that dominates in dynamic stall starts at the leading edge of the blade with the development of a vortex. This vortex moves

downstream across the blade in the direction of the air flow. In the process, far higher C_l , C_d and C_m values act than would be possible in the steady case. Before the vortex separates at the trailing edge, the lift reaches a maximum. As the vortex separates, however, very strong negative pitch moments occur. The separated airflow is now fully developed and, if the blade has again reached a low angle of attack in its oscillatory motion, it takes much longer for a "healthy" flow pattern to be restored. The strong pitch moments act via the control rods to produce vibration in the helicopter airframe.

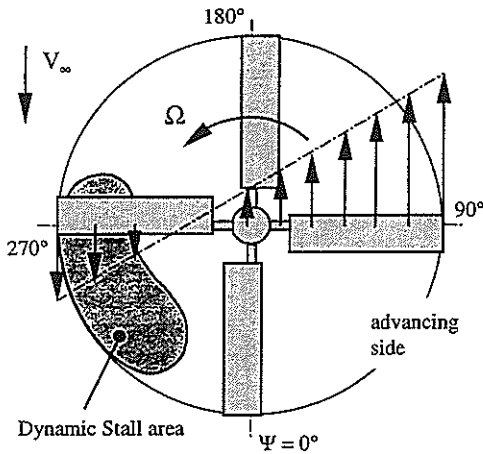


Fig. 1 Velocity vectors and dynamic stall area on the rotor disk in forward flight.

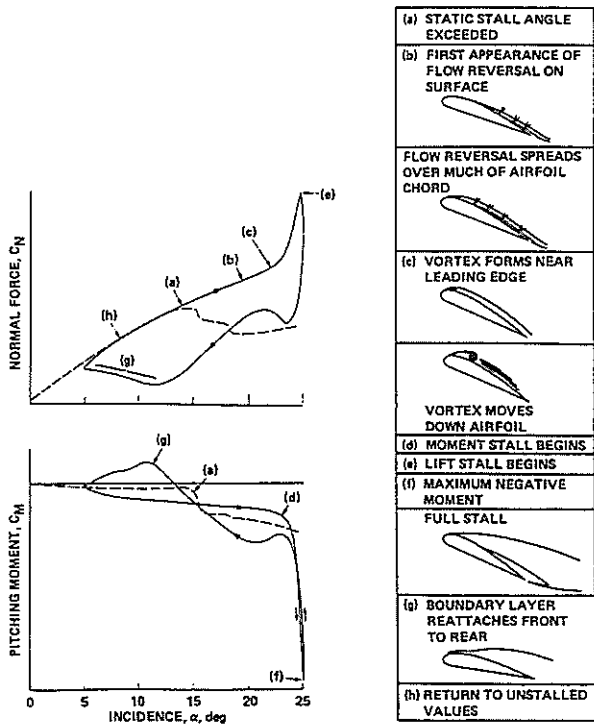


Fig. 2. Dynamic stall processes on the NACA 0012 airfoil (dashed lines represent static values) [4]

3. DYNAMIC HIGH-LIFT DEVICES

It is assumed that high-lift devices, as have been used successfully on fixed-wing aircraft, can, to a certain extent, be applied to helicopters as well [6]. The known measures can be divided into two groups: airfoil geometry variation and direct influence of the boundary layer. Measures that only ensure a delay of the flow separation by statically altering the airfoil properties are not considered here. These methods generally provide higher lift on the retreating side of the rotor but can cause disturbances at higher Mach numbers (higher drag, induction of shocks). To prevent negative effects, a dynamic process is required.

The work by McCloud et al. [7] was one of the first successful attempts to actively and dynamically influence blade characteristics in this way. In full-scale wind-tunnel tests, they succeeded in delaying flow separation on the retreating blade by blowing air tangentially into the boundary layer through small slits near the leading edge ($x/c=0.085$) on the upper side of the airfoil. First air was blown continuously on all the blades. By suitable control in the distributor for blowing on the retreating blade only, the mass flow, and thus the required power, was reduced by one half without any loss of the positive effect. Experiments in which blowing was carried out further downstream on the airfoil showed no effect. The above-described local limitation of the dynamic stall phenomenon to effects on the leading edge of the blade and in the retreating blade area is evident. In principle, tangential acceleration of the boundary layer fluid across the upper side of the airfoil also occurs with a slat, but in this case the air is taken from the bottom side of the airfoil and guided through a converging gap to the top. A moveable slat [8] or a gap, with a stationary leading-edge section, that is dynamically opened and closed [9] have been proposed.

A number of studies exist on dynamic geometry variations. The approaches range from a simple thickness variation of a symmetrical airfoil [10], to a dynamic increase of airfoil camber achieved by lowering the leading edge of the blade (nose droop) [11], [12], to a consideration of the influence of the airfoil nose radius [13], [14]. What they all have in common is a positive effect on delaying the dynamic stall onset. Continuous deformation of the blade contour has decisive aerodynamic advantages. Even very small changes produce an effect, especially in the sensitive leading-edge area.

From the multitude of the alternatives described above, the approach using a discrete leading-edge flap was selected. The positive aerodynamic effect of dynamically lowering the leading-edge of an airfoil (nose droop) had already been successfully demonstrated on various airfoil geometries. The high negative-pressure peaks at the leading edge are reduced, flow separation is delayed, and hysteresis loops are reduced. A discrete flap also permits the energy required for elastic deformation during continuous contour variation to be used to overcome the aerodynamic forces and moments or to provide greater movement authority. Based on existing flap technologies, integration in a rotor blade appears feasible.

4. ACTUATOR TECHNOLOGY

To operate a dynamic high-lift device, a actuation mechanism of some sort is needed. Systems that require extensive auxiliary components should be avoided from the outset. Local integration in the rotor blade itself places extreme demands on the system: very limited installation space, large centrifugal loads, highly dynamic control, high performance, and low weight. A promising approach is offered by actuators based on piezoceramic materials.

The characteristics of piezoceramic actuators are based on the inverse piezoelectrical effect. Piezoceramics are solid-state materials that change in shape when subject to an electric field. Their use as sensors is well known. In such applications, a mechanical deformation is converted into a voltage by internal charge shifts [15]. This combined ability makes piezoceramic elements ideal for integrated adaptive electromechanical systems. Thanks to their solid-state characteristics, very high forces, high precision, and high dynamics can be achieved. However, the small deflections must be amplified if these elements are to be used advantageously in macroscopic systems. The Research & Technology Department of DaimlerChrysler has successfully introduced several hybrid actuator systems that meet these requirements [16].

The double frame developed for flap actuation shown in Fig. 3 amplifies the displacement of the piezostack by a factor of about 10. The generated force is correspondingly reduced in accordance with the leverage law.

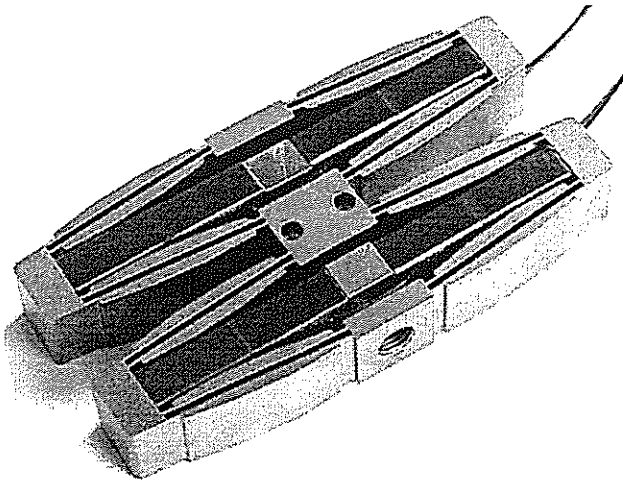


Fig. 3. Hybrid actuator with double transmission frame and integrated piezostacks.

This arrangement ensures absolutely playfree operation and only relatively small energy losses in the bending zones. Characteristic parameters of this actuator are a blocking force of 650 newtons with a free displacement of 1.10 mm. Easy scaling of these value allows custom-made design for different fields of application. Additionally piezoceramic actuators as relatively modern devices offer high potential for future improvements [16]. The high power density permits complete integration in the rotor blade contour. Only three lines through the blade are required for power supply, and the energy can be transmitted from the rotor to the nonrotating system via conventional slip rings.

5. NUMERICAL SIMULATIONS

The numerical simulations were performed with a conventional rotor-blade airfoil of medium relative thickness as used in modern helicopters. It represents an ideal compromise for use in current helicopters. To ensure a continuous data base this airfoil geometry is used throughout all subareas of AROSYS. However, it has certain deficiencies for investigating the dynamic stall effect, e.g. a relatively high camber in the leading-edge area. Nevertheless, these aspects are secondary to the demonstration of design feasibility. In principle, the system can be integrated in any airfoil providing the same installation volume.

The primary considerations for determining the flap dimensions are the aerodynamic efficiency together with the moments resulting from the necessary geometry variation and the forces acting on the actuators. In aerodynamic terms, a large flap with a large deflection is desirable. However, this desire places considerable demands on the actuators. Thus, here too the object is to find an optimum compromise. The numerical simulations consider only the two-dimensional case.

The first step is to generate suitable geometries. The pivot position x_0/y_0 is varied as well as the deflection angle η_f with intermediate steps at increments of 0.5° . From the pivot, a projection is made perpendicular to the upper side of the airfoil in order to define the end of the flap. A radius then begins at this point, which at the maximum deflection describes a gentle transition to the rest of the airfoil. The discontinuity in the contour of the bottom of the airfoil has no effect on the accuracy of the result. With the specified coordinates, the simulation tool used generates a new "interpolated" contour that exhibits a smooth transition (Fig. 4). The discussions in the further course relate to a pivot position in the y-direction that is always on the bottom side of the airfoil. This has three main advantages: a simplified method of geometry generation, maximum curvature radius at the transition area, and minimal influence on the aerodynamic effect.

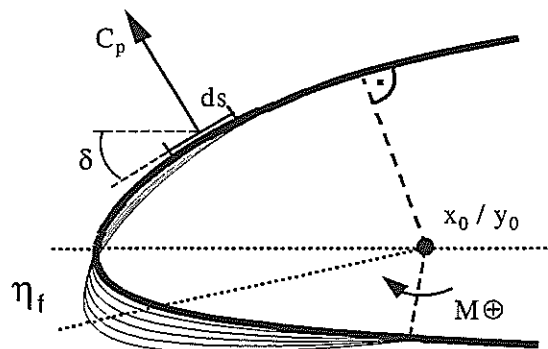


Fig. 4. Generation of the nose flap geometry.

For the aerodynamic simulations, three reference points were defined that are derived from one case of fast forward flight (TABLE 1). Here, case 1 is of main importance. Cases with higher Mach numbers were also investigated but are not discussed further. They are of interest with respect to "nonoperation" in the neutral position.

Case	Ma	Re	Ψ [°]	
1	0.33	2.29e6	270	Retreating blade
2	0.54	3.74e6	0 / 180	
3	0.74	5.13e6	90	Advancing blade

TABLE 1. Reference points for simulation (fast forward flight, $\mu = 0.37$)

For simulation, a program package was used which is based on the solution of Euler's equation with boundary-layer coupling [17]. The results obtained included the pressure distribution and the integral coefficients. From the pressure distribution, also the loads on the flap were calculated. Integration was then performed only over the flap surface with the pivot x_0, y_0 as a reference point (Fig. 4). Selective consideration of the friction coefficient c_f produced only fractions of the integral forces and moments of less than 3% and is not further pursued here. For faster convergence, a forced transition was set at $x/c=0.06$.

Fig. 5 shows the maximum lift coefficient of the airfoil as a function of the flap geometry. With increasing relative flap size x_f/c and increasing deflection angle η_f , an approximately linear growth of $C_{l,max}$ can be observed. However, with small flap geometries, the curve flattens at larger angles. Increasing the flap angle then does not result in any further growth of $C_{l,max}$. A limitation of the flap size and flap deflection due to the resulting loads acting directly on the actuators occurs relatively quickly.

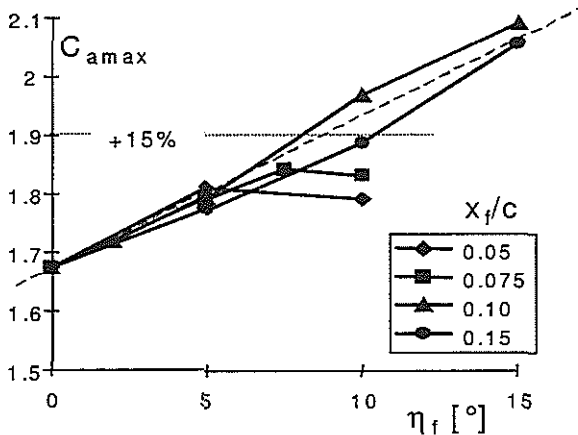


Fig. 5. Maximum lift coefficients for various flap configurations (case 1).

Fig. 6 presents the moment coefficient of the flap in relation to the flap pivot for various flap geometries on the original airfoil (flap in the neutral position). It can be seen that the moment coefficient is relatively independent of the pivot position in the y -direction in comparison to the flap size. A special feature is the possibility of moment-neutral mounting of the flap for a relative airfoil fraction of about 7.5%. However, such a small flap would not be very useful. Fig. 7 shows the dependence of the moment coefficient of the flap c_{mf} on the deflection angle η_f for a

flap of 10% relative airfoil chord. The growth of the acting moment is smaller than that resulting by shifting the pivot position. The cluster of curves with open symbols shows the limits for an actuator with various levels of performance. The following applies to the hybrid actuator used here:

$$F_B \frac{s}{2} = 650N \cdot 0.55mm = 0.35Nm$$

Fig. 8 shows for the reference cases defined in TABLE 1 with the established flap size the expected moments that act on the actuators via the mechanism as forces to be overcome. It is noteworthy in this context that the coefficients for various Mach numbers are virtually identical over a large angle-of-attack range. For the maximum deflection, the moment increases further at high angles of attack. At lower angles of attack the moment acting on the flap becomes negative. This means that the actuators must hold the flap, for example on the advancing side, in the neutral position.

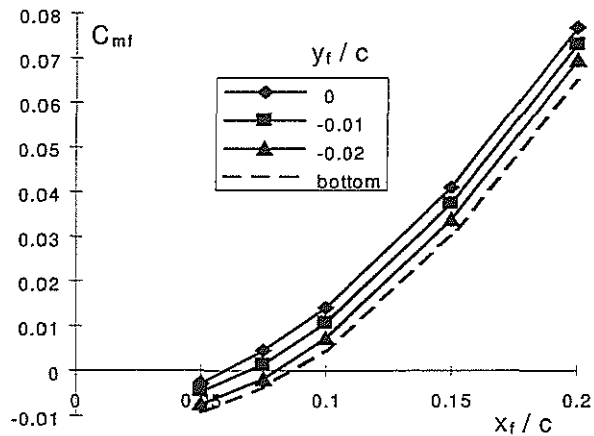


Fig. 6. Flap moment coefficient on the original airfoil as a function of pivot position and thus flap size (case 1, $\alpha=12.5^\circ$).

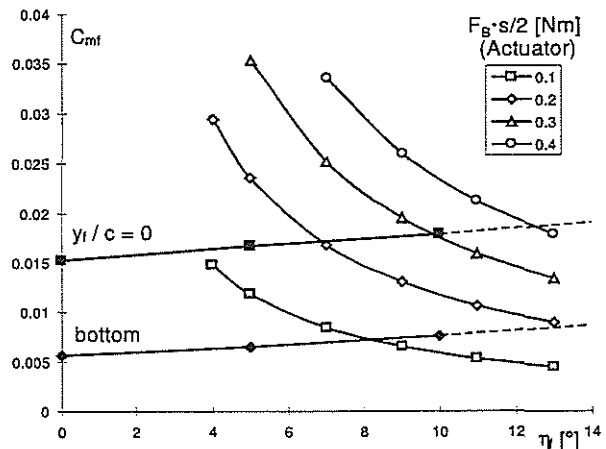


Fig. 7. Moment coefficient as a function of pivot position and flap angle in comparison to the performance of the actuator.

Thus, a flap size of 10% relative airfoil chord and 10° maximum deflection seems feasible. For this configuration the maximum lift coefficient increases by 17%. The angle of attack at which drag increases significantly and the stall angle are increased by about 2.5° (Fig. 9).

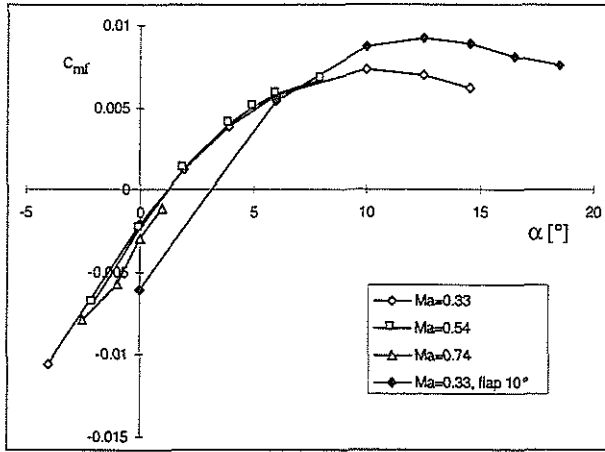


Fig. 8 Moment coefficient of the nose flap on the original airfoil for cases 1–3 and for the maximum deflection angle of the flap in case 1 versus angle of attack.

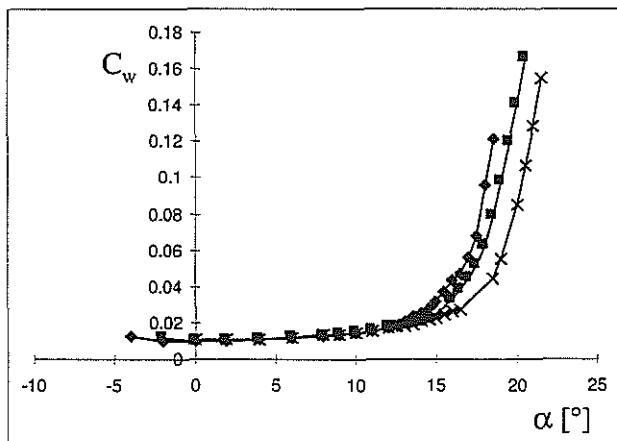
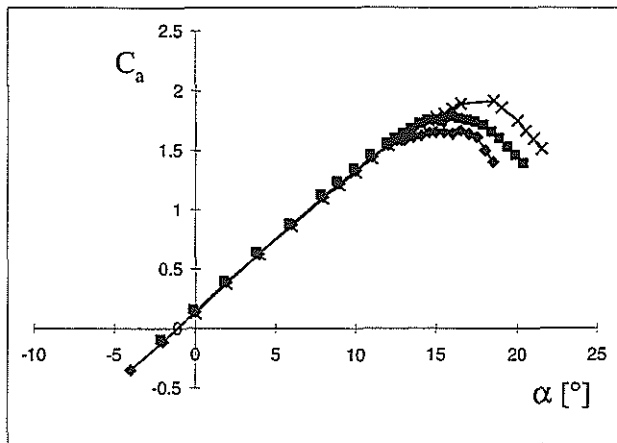


Fig. 9 Lift, resistance, and moment coefficients versus angle of attack for the original airfoil and with lowered nose flap (case 1).

6. STRUCTURAL DESIGN

General aspects for the structural implementation are shown in Fig. 10. To ensure a smooth airfoil contour at rest as well as in the deflected position, special attention must be given to the precise implementation of the interface from the flap to the trailing airfoil structure. The integratability and exchangeability of the erosion protection must also be considered. Here, a discrete flap has decisive advantages, as erosion protection can continue to be realized as before. All joints and connections must be free of play and as frictionless as possible.

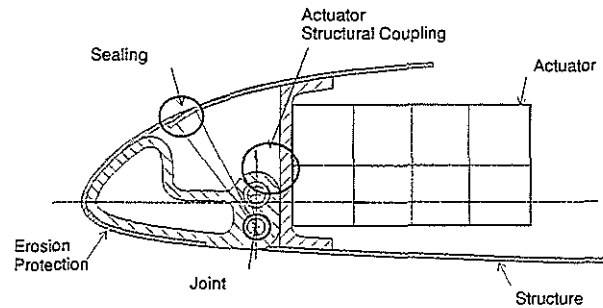


Fig. 10. General design aspects for implementation of the leading-edge flap for adaptive airfoil variation.

The assumptions made in the numerical simulations with regard to the pivot position cannot all be realized in the design of the flap. Fig. 11 schematically illustrates the functional principle. Asymmetric forces on the actuators should be avoided. Due to the installation height of the actuator, the line of action approximately coincides with the zero line of the airfoil ($y/c=0$). The paired actuators are arranged in series. The structural attachment is located in the center between the two frames. To monitor the force level and to characterize the system, two axial force transducers are initially integrated in the load path. However, these will not be integrated in the actual helicopter rotor blade, where the preload level will be set purely by means of geometric relationships.

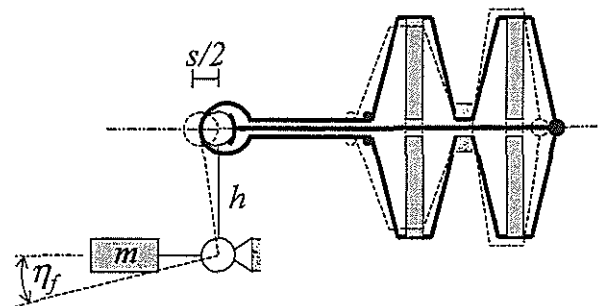


Fig. 11. Principle of the mechanism of action of the leading-edge flap.

By applying an offset voltage of half the maximum voltage to the piezostacks, the system is endowed with an additional preload. The actuators are wired in such a way that they always move in push-pull mode. For example, if the rear piezostack elongates, the transmission frame undergoes contraction in the direction of its width. This

movement is transmitted via the rear coupling point to the push rod. The rod extends through the entire arrangement to the front, where it causes a forward movement of the flap pivot. This leads to a downward deflection of the flap via the lever arrangement. The other piezostack contracts, producing a movement of the pull rod in the same direction via the frame. The adjusted force level remains constant in the process (ignoring losses). Deflection of the flap in the other direction, i.e. upward, is undesirable and is therefore prevented by a stop. Since no displacement is needed in this direction, a much higher force authority is available (blocking force) to keep the flap in the neutral position on the advancing side of the rotor (see Fig. 8).

The flap is hinged on high-precision ball-bearings. These only have to withstand the relatively small transverse aerodynamic forces. In order to maintain the required deflection angle of 10° in the context of the available displacement authority of the actuator of $s/2=0.55$ mm, a lever arm of 3.15 mm was selected. The small dimensions demand high-precision manufacturing of all the components. Particularly at the interface of the flap to the rest of the blade, care must be taken to ensure that no excessive gaps or steps occur. The curved surfaces will help to maintain a relatively high stiffness of the components. Fig. 12 shows the demonstrator built for test purposes. The voluminous force transducers will not be present when the mechanism is integrated in an actual rotor blade. The actuators can then be moved forward by about 40 mm. This will result in a weight reduction while at the same time helping to keep the center of gravity line of the airfoil at 25%. In current airfoils, this is usually accomplished by integrating lead in the nose section. With a moving leading-edge flap, such a high weight within the flap would be disadvantageous. The leading-edge flap must be as lightweight as possible.

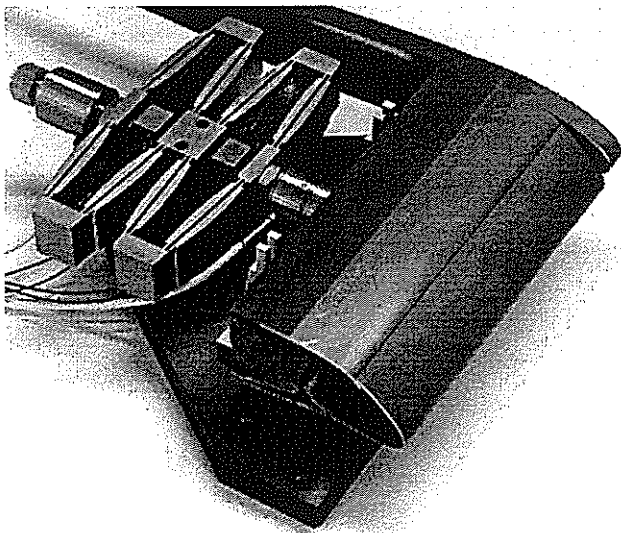


Fig. 12. Demonstration model for functional analysis of the leading-edge flap.

7. CONCLUSION AND OUTLOOK

The performance of current helicopters is limited by the occurrence of dynamic stall on the retreating side of the rotor. This situation may be remedied by the use of dynamic high-lift devices integrated in the rotor blades. From

the large number of possibilities available, an approach was selected that appears suitable for implementation with reasonable effort: dynamic lowering of the leading edge of the blade by means of a discrete flap (nose droop). The discrete leading-edge flap has several advantages. Experience gained from the implementation of the discrete trailing-edge flap (servoflap) can be directly applied. The simple defined geometry variation, the already demonstrated efficiency, and the clear mechanical aerodynamic relationships further facilitate the design process. Numerical simulations led to a compromise between the aerodynamic efficiency resulting from the flap size and deflection and the resulting loads on the actuators. For a 10% flap with 10° maximum deflection angle, a 17% increase of the maximum lift and a 2.5° shift of the stationary stall angle were achieved at a low Mach number.

High-performance actuators based on piezoelectrical materials have been chosen as drives for the flap. Piezoactuators are distinguished by a high power density and, thanks to their specific properties, are superior to conventional approaches under the given conditions. An amplification frame makes their elongation at a high force level practicable for macroscopic applications. All interfaces are free of play and as frictionless as possible. Both the aerodynamic design and the structural implementation were limited to the two-dimensional case, which is sufficient for the planned wind-tunnel tests. The model discussed is intended to demonstrate the basic feasibility of structural integration.

For helicopter use, other important conditions must be taken into account. Here, we can draw upon the experience gained with the much further developed servoflap. Important points are a design suitable for rotational use, three-dimensional effects, and failsafe operation. A new, optimized design of the entire rotor system based on the assumption of the availability of integrated control surfaces has great potential. Thus, for example, the airfoil thickness in the outer blade area could be reduced. The resulting reduced lift could be compensated for by means of dynamic high-lift devices with a simultaneous power saving and possible reduction of high-impulsive noise. Combined use with a servoflap would also be conceivable. Considerable potential for improvement is thus available for future helicopter generations.

8. REFERENCES

- [1] Martin, W., Jänker, P., Lorkowski, T., Neumann, H., Hübner, M., Leitkonzept Adaptive Rotorsysteme – Neue Technologien zur adaptiven Blatt-Geometrie und Sensorik, DGLR Jahrestagung, Bremen, 1998
- [2] Schimke, D., Jänker, P., Wendt, V., Junker, B., Wind Tunnel Evaluation of a Full Scale Piezoelectric Flap Control Unit, TE02, 24th European Rotorcraft Forum, Marseilles, 1998
- [3] McCroskey, W.J., The Phenomenon of Dynamic Stall, NASA TM-81264, 1981
- [4] Carr, L.W., McAlister, K.W., McCroskey, W.J., Analysis of the Development of Dynamic Stall on

- Oscillating Airfoil Experiments, NASA TN D-8382, January 1977
- [5] Geissler, W., Vollmers, H., Unsteady Separated Flows on Rotor Airfoils, 18th European Rotorcraft Forum, Avignon, September 15-18, 1992
- [6] Yu, Y.H., Lee, S., McAlister, K.W., Tung, C., High Lift Concepts for Rotorcraft Applications, 49th American Helicopter Society Annual Forum, St. Louis, May 19-21, 1993
- [7] McCloud, J.L., Hall, L.P., Brady, J.A., Full-Scale Wind-Tunnel Tests of Blowing Boundary-Layer Control Applied to a Helicopter Rotor, NASA TN D-335, September 1960
- [8] Tung, C., McAlister, K.W., Carr, L.W., The Quest for Stall-Free Dynamic Lift, Workshop on Physics of Forced Unsteady Separation, Moffet Field, April 17-19, 1990
- [9] Ruffin, S.M., Mavris, D.N., Application of Dynamic Slot and Circulation Control Technologies to Rotors for Noise reduction and Dynamic Stall Elimination, Georgia Institute of Technology Research Proposal, 1997
- [10] Geissler, W., Raffel, M., Dynamic Stall Control by Airfoil Deformation, 19th European Rotorcraft Forum, Cernobbio, September 14-16, 1993
- [11] Geissler, W., Sobieczky, H., Dynamic Stall Control by Variable Airfoil Camber, AGARD FDP Symposium on Aerodynamics and Aeroacoustics of Rotorcraft, Berlin, October 10-13, 1994
- [12] Lee, S., McAlister, K.W., Tung, C., Characteristics of Deformable Leading Edge for High Performance Rotor, AIAA-93-3526, AIAA 11th Applied Aerodynamics Conference, Montgomery, August 9-11, 1993
- [13] Geissler, W., Carr, L.W., Chandrasekhara, M.S., Wilder, M.C., Sobieczky, H., Compressible Dynamic Stall Calculations Incorporating Transition Modelling for Variable Geometry Airfoils, AIAA-98-0705, AIAA 36th Aerospace Sciences Meeting and Exhibit, Reno, January, 12-15, 1998
- [14] Chandrasekhara, M.S., Wilder, M.C., Carr, L.W., Control of Flow Separation Using Adaptive Airfoils, AIAA-97-0655, AIAA 35th Aerospace Sciences Meeting and Exhibit, Reno, January 6-10, 1997
- [15] Koch, J., Piezooxide – Eigenschaften und Anwendungen, ISBN 3-7785-1755-4, Valvo Unternehmensbereich Bauelemente der Philips GmbH, Hüthig Verlag, Heidelberg, 1. Auflage, 1988
- [16] Jänker, P., Hermle, F., Lorkowski, T., Storm, S., Christmann, M., Wettemann, M., Development and Evaluation of Advanced Flap Control Technology Utilizing Piezoelectric Actuators, 25th European Rotorcraft Forum, Rome, September 1999
- [17] Drela, M., Giles, M.B., ISES: A Two-Dimensional Viscous Aerodynamic Design and Analysis Code, AIAA-87-0424, AIAA 25th Aerospace Sciences Meeting, Reno, January 12-15, 1987